On-Board Particulate Filter Failure Prevention and Failure Diagnostics using Radio Frequency Sensing

Author, co-author (Do NOT enter this information. It will be pulled from participant tab in MyTechZone)

Affiliation (Do NOT enter this information. It will be pulled from participant tab in MyTechZone)

Abstract

The increasing use of diesel and gasoline particulate filters requires advanced on-board diagnostics (OBD) to prevent and detect filter failures and malfunctions. Early detection of upstream (engine-out) malfunctions is paramount to preventing irreversible damage to downstream aftertreatment system components. Such early detection can mitigate the failure of the particulate filter resulting in the escape of emissions exceeding permissible limits and extend the component life. However, despite best efforts at early detection and filter failure prevention, the OBD system must also be able to detect filter failures when they occur. In this study, radio frequency (RF) sensors were used to directly monitor the particulate filter state of health for both gasoline particulate filter (GPF) and diesel particulate filter (DPF) applications. The testing included controlled engine dynamometer evaluations, which characterized soot slip from various filter failure modes, as well as on-road fleet vehicle tests. The results show a high sensitivity to detect conditions resulting in soot leakage from the particulate filter, as well as potential for direct detection of structural failures including internal cracks and melted regions within the filter media itself. Furthermore, the measurements demonstrate, for the first time, the capability to employ a direct and continuous monitor of particulate filter diagnostics to both prevent and detect potential failure conditions in the field.

Introduction

Particulate matter (PM) emissions from diesel and gasoline engines have come under increasing regulatory scrutiny over the past decade. PM emissions from on-road diesel engines are limited to no more than 0.01 g/hp-hr (0.013 g/kW-hr) in the United States and 0.01 g/kW-hr in the European Union, which also imposes a particle number limit [1, 2]. The Euro 6 standards limit particle number emissions to no more than $6.0x10^{11}$ particles/km by 2018 [3] which impacts both diesel and gasoline engines.

Efforts to meet these regulations have converged on the use of particulate filter technologies, primarily cellular ceramic filters for diesel engines (DPF) and are increasingly being applied to reduce PM emissions from gasoline direct injection engines (GPF) in some applications. Standards similar to those mandated by the U.S. and E.U. are being phased in around the world (to varying degrees), and include off-road, mobile and stationary engines as well.

Properly functioning (healthy) particulate filters are extremely effective at trapping and reducing engine-out PM emissions, and may achieve trapping efficiencies of 99% or more in some cases. However, actual in-use conditions may exist which can compromise filter operation. Ensuring proper particulate filter operation and detection of malfunctions of the system on the vehicle is critical in order to meet additional on-board diagnostics (OBD) requirements. OBD requires the detection of filter failures or malfunctions on the vehicle, which could lead to tailpipe PM levels exceeding some predefined multiple of the emissions limit [4-5]. These OBD requirements have further motivated the development of physical and virtual (model-based) sensors and algorithms to detect particulate filter failure conditions. Nonetheless, accurate detection of filter failures to meet OBD limits is a challenge.

In addition to filter diagnostics, accurate determination of the particulate filter loading state is important for safe and efficient operation of the engine and aftertreatment system. The accumulation of PM in the filter results in increased exhaust flow restriction with a direct impact on engine efficiency. The accumulated PM may be removed from the filter through active or passive oxidation processes to maintain exhaust backpressure at acceptable levels. Active soot oxidation (regeneration) requires the consumption of additional fuel in order to increase exhaust temperatures to initiate and sustain soot oxidation in the particulate filter [6].

In order to protect the filter, it is important to ensure the PM does not accumulate above an acceptable level, defined as the soot mass limit, in order to avoid excessively high temperatures during regeneration which may result in filter failures due to melting or cracking [7]. Indeed, the majority of filter failures are typically the result of either an upstream failure or malfunction of the engine such as a malfunction of the EGR, turbo-charger, injection system, or similar sub-system resulting in high engine-out PM, or a failure of the sensing and control system to accurately determine the filter loading

This manuscript has been authored by Filter Sensing Technologies, Inc., a subsidiary company of CTS Corporation and is based upon work supported by the U.S. Department of Energy DE-EE0005653.

level. The result of both of these malfunctions to either the engine or aftertreatment sensing or control system is often manifested as an uncontrolled regeneration event, resulting in physical damage to the filter and a potential loss in filtration efficiency. Typical failure modes due to these sources include the formation of radial cracks (so-called "ring-off cracks"), melt regions in the filter, or the fracture of the material and loss of channel end-plugs in some cases [8]. In all cases the aim of the combined engine and aftertreatment control system if to avoid these types of failures under all conditions. However, should such a failure occur, the OBD system must detect conditions which may result in PM emissions above acceptable levels.

Conventional Approaches

Current methods for managing particulate filter operation rely on an indirect approach utilizing filter pressure drop measurements, so called delta-P sensors, to deduce the filter soot load from the exhaust flow restriction due to the accumulated soot. A schematic of the system is shown in Figure 1. The accuracy of this approach depends heavily on the flow conditions at the time of the measurements, and there are a number of operating conditions over which accurate pressure drop measurements are not possible, including: (i) low flow rate such as idle, and (ii) highly transient operation with large fluctuations in flow and pressure drop.

In other cases, including during regeneration, the dynamics of the soot oxidation (whether occurring in the pores or on the filter cake layer) also introduce considerable variability in the pressure drop measurements, including well-known hysteresis effects [11]. Such effects occur in both active and passively regenerated systems. In one example, studies at Oak Ridge National Laboratory reported pressure drop levels returning to nearly clean levels with over half of the soot remaining in the filter during regeneration [12]. The use of predictive models, in addition to pressure measurements, can improve the overall accuracy of the pressure-based estimates in some cases, however without direct feedback these approaches are not able to adapt to conditions outside the bounds of the initial model calibration.

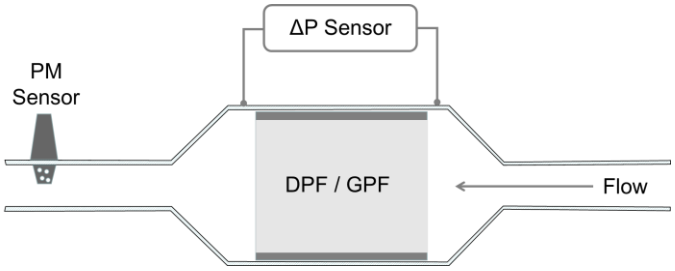

Figure 1. Conventional particulate filter monitoring configuration consisting of a pressure drop sensor and downstream PM sensor.

Following regeneration, a small amount of incombustible material or ash is left behind. The ash, primarily composed of inorganic metallic components derived from engine oil additives, including detergents and anti-wear additives also accumulates in the filter over time [9]. Ash accumulation further restricts exhaust flow through the filter and contributes to an increase in pressure drop, which further complicates pressure-based control systems. Depending on the location of the ash deposits, the ash may also enhance the filtration efficiency (particle capture) of the filter by serving as an added filtering medium along the channel walls [10].

For many of the reasons outlined above, OBD requirements are challenging for pressure- and model-based approaches. As a result, soot sensors have been developed to detect soot which may pass through the particulate filter, as a result of a filter failure. Various types of sensors exist but can be broadly defined by two categories: (i) accumulating electrode sensors, and (ii) electric charge-based sensors [13]. Accumulating electrode type sensors function in a similar manner to the particulate filter, by monitoring a change in the electrical properties (typically resistance) on an electrode due to soot deposition. The electrode is periodically heated to regenerate (oxidize) any accumulated soot. In this manner accumulating electrode type sensors do not provide a real-time measurement of exhaust soot levels, but rather a time averaged measurement between sensor regeneration events [14]. Charge-based sensors, on the other hand, operate by inducing a charge on the incoming soot particles and monitoring that charge to determine the soot emissions rate [15]. In either approach, the current state-of-the-art for particulate filter control and OBD relies on the use of indirect estimates of the filter loading state from pressure-drop measurements and predictive models, along with downstream soot sensors to detect soot leakage from the particulate filter only after the filter has failed. Recent work has also indicated the inability of resistive approaches to accurately monitor tailpipe soot emissions from gasoline engines [16].

Radio Frequency Sensing

In contrast to current approaches, this work utilized radio frequencies (RF) to directly interrogate and monitor the state of the particulate filter. The operation of the system for directly monitoring soot and ash levels on the filter has been described in detail in previous publications [17-19]. The measurements rely on the use of the metallic filter housing as an RF resonant cavity. Accumulation of particulate matter on the filter alters the dielectric properties of the resonant cavity and enables direct measurement of the particulate filter soot loading level, provided the filter media is non-conducting (transparent to RF). Similar RF-based approaches have also been applied to catalyst systems including selective catalytic reduction (SCR) and three-way catalysts (TWC) to monitor ammonia loading and oxygen storage, respectively [20-21]. Figure 2 provides an illustration of the RF system configuration used in this study where two probes are used to transmit and receive an RF signal in the filter housing. The RF signal propagates through the ceramic filter thereby providing a direct measurement of the filter's state.

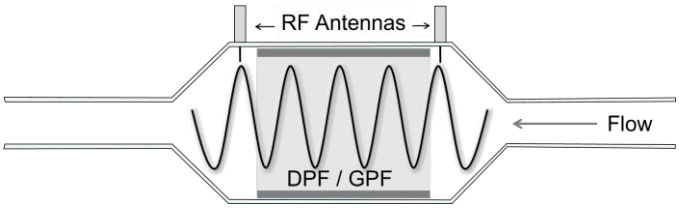

Figure 2. RF measurement system configuration showing two antenna probes used to transmit and receive the RF signal as well as the signal propagating through the ceramic filter media within the housing.

Other configurations of the system shown in Figure 2 are possible, inlcuding the use of only a single antenna, where the same antenna is used to transmit and receive the RF signal. A benchmarking study using a single antenna RF system to control DPF regeneration relative to the stock pressure- and model-based controls was previously reported to result in 15% to 30% shorter regenerations due to direct feedback of the soot oxidation during regeneration from the RF sensor [19]. Results of fleet durability testing of RF measurements systems with several Volvo/Mack vehicles also showed similar results [18].

Transmitting an RF signal over a broad frequency range within a metallic filter housing results in the resonance response shown in Figure 3. The peaks in the curves correspond to specific resonant modes, characteristic of the cavity, which are influenced by the dielectric properties of the material residing therein (filter, soot, ash). The figure shows a clear and distinct difference between an empty filter housing and one that contains a filter, which results in a shift of the resonances to lower frequencies. In this manner the presence (or absence) of the filter from the housing is readily detected. The same approach is applicable to catalysts.

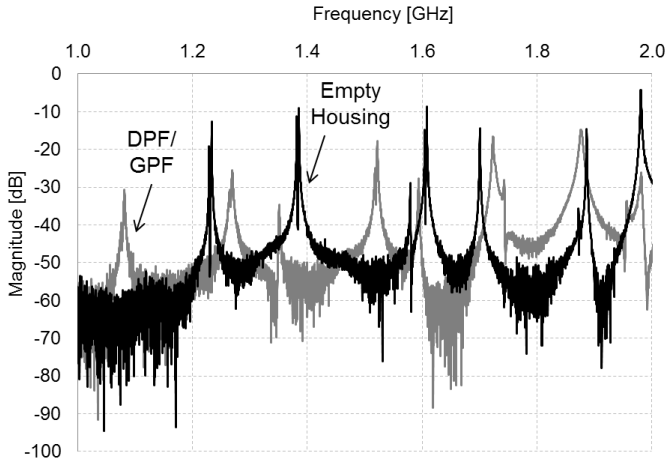

Figure 3. RF response for empty filter housing (black curve) and filter housing containing ceramic filter element (DPF/GFP).

The measurements corresponding to the results in Figure 3 were conducted with no flow through the system (engine off). In contrast to current approaches using pressure or temperature sensors to detect the presence of the filter or catalyst, which requires the engine be on and generating sufficient exhaust flow for a measurement, the RF measurements may be carried out at any time over the course of the drive cycle, including with the engine off.

Previous work has described the impact of soot and ash accumulation in the filter on the RF signal response, which serves to reduce the amplitude of the resonances (due to the high dielectric loss of the soot) and impacts the resonance frequency (in the case of ash) [17-19, 22]. In all cases the presence or absence of the filter, shown in Figure 3, exerts a change in the RF signal far greater than normal soot or ash loading, and can thus be readily distinguished from normal filter operation.

Examples of the impact of various intentionally induced filter failure modes on the RF signal response are shown in Figures 4-7. A series of successively deeper cuts (in the radial direction) to the back surface of the filter is shown in Figure 4, which had the effect of removing an increasing number of ceramic end-plugs from the back of the filter. The corresponding RF measurements are shown in Figure 5 for one particular resonant mode. As can be seen from the measurements, the removal of ceramic material from the filter, such as the removal of end-plugs, results in a shift to higher resonant frequencies. The shift to higher frequencies with the removal of filter material from the housing is further consistent with the results in Figure 3, which show a large shift to lower frequencies as the filter was added to the cavity, relative to the empty cavity measurements.

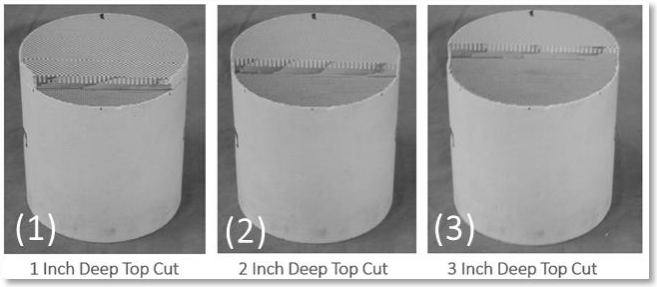

Figure 4. Defects introduced to new cordierite filter by cutting and increasing number of ceramic end plugs off of the back face of the filter.

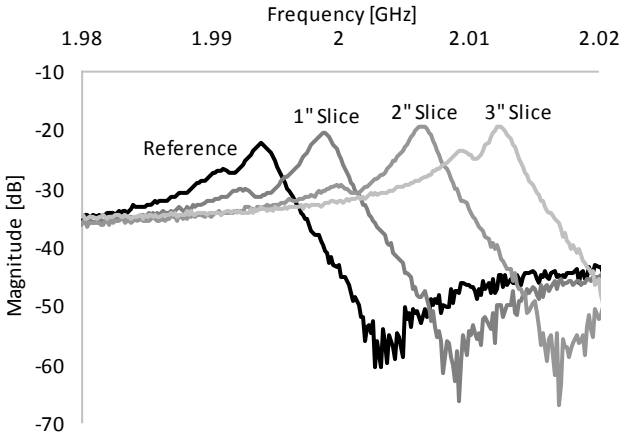

Figure 5. RF response of new filter and impact of increasing severity of defect introduce to back face of ceramic filter on RF signal.

Similar experiments were conducted, as shown in Figure 6, where a radial cut was made near the center of the DPF, with increasing thickness (depth of cut). The corresponding RF measurements are shown in Figure 6 for another resonant mode. Similar to the results in Figure 5, the removal of ceramic material from the filter results in a shift in the resonant frequency to higher frequencies.

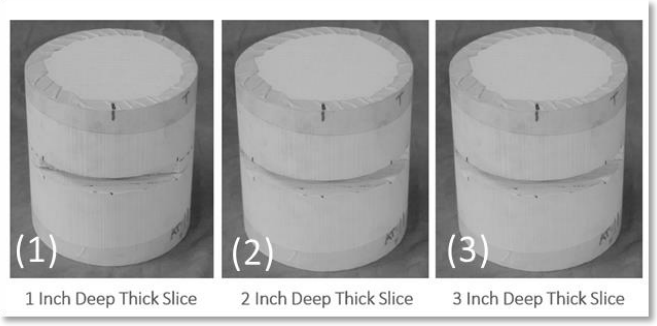

Figure 6. Defects introduced to new cordierite filter by cutting a slice from the center of the filter of increasing depth from 1 to 3 inches.

The sensitivity of a particular resonant mode to a specific local defect is dependent on the local electric field strength of that particular mode. Each resonant mode is associated with a specific electric field distribution in the filter, and monitoring multiple modes enables different regions of the filter to be interrogated spatially. The results of experiments and simulations evaluating the electric field distribution within the filter housing for a particular configuration are reported in [23]. Figure A-1 of the Appendix presents several

examples of the simulation results showing the electric field distribution for different resonant modes, corresponding to a cordierite gasoline particulate filter application.

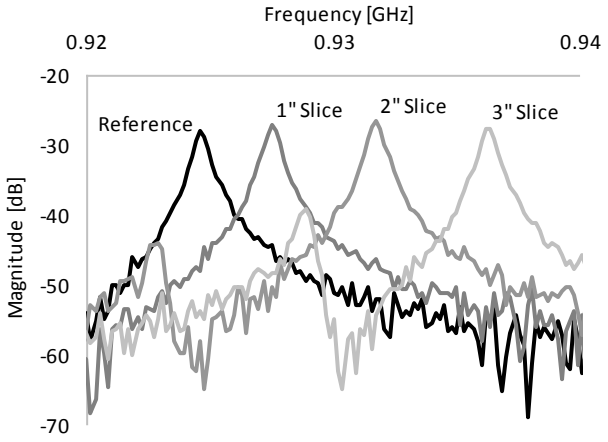

Figure 7. RF response of new filter and impact of increasing severity of defect introduced to center of ceramic filter on RF signal.

Figures 3, 5, and 7, thus indicate the potential to not only detect the presence or absence of the filter (or other ceramic substrate) within the exhaust aftertreatment system, but also indicate the sensitivity of the RF measurements to local defects. The measurements may further be carried out during normal operation, or even with the engine off (no exhaust flow) as shown in the figures.

Experimental Approach

Given this discussion on the background and fundamental operating principles of the RF measurements, the remainder of this work is focused on evaluating specific diagnostic applications of the RF sensing technology. It was the aim of this study to first detect signs of upstream (of the DPF/GPF) malfunctions in order to provide early warning/prevent catastrophic filter failure, and second to evaluate the accuracy of the RF measurements to detect a reduction in filter trapping efficiency should damage to the filter have occurred. The experimental results span heavy-duty vehicle tests as part of a three-year field trial as well as laboratory dynamometer evaluations on diesel and gasoline engine applications conducted at Oak Ridge National Laboratory's Fuels, Engines and Emissions Research Center.

RF Sensor

The RF sensor utilized in this study consists of a sensor control unit and a measurement probe, shown in Figure 8. The measurement probe, a stainless steel rod-type antenna, is a passive component used to transmit and receive the radio-frequency signals in the filter housing. The antenna is of similar size and form factor to conventional temperature sensors used in exhaust systems. The control unit contains the RF electronics as well as an embedded micro-controller. A wiring harness connected to the unit, provides additional inputs from exhaust temperature sensors for temperature compensation of the RF signal. The measurement output is broadcast via the CAN network.

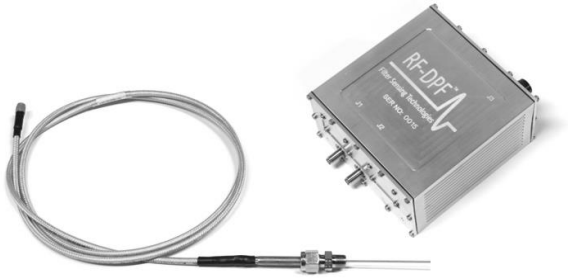

Figure 8. RF measurement system including sensor control unit and measurement probe.

The RF sensor, shown in Figure 8 provides fast response, less than 1 second, measurements of filter soot levels, enabling near real-time filter management. Unlike conventional pressure sensors, the RF sensor is unaffected by exhaust flow rate [17], but does require temperature compensation, as the dielectric properties of the PM do vary with temperature. The sensor is capable of accurately measuring soot in the DPF over the full range of engine operating conditions spanning idle to high temperature active regeneration events, including drop-to-idle, as previously reported [22].

Results of RF sensor evaluations on a 1.9L GM turbo-diesel engine at Oak Ridge Laboratory are presented in Figure 9. The evaluations explored sensor response time relative to AVL Microsoot Sensor (MSS) measurements of engine-out soot. Figure 9(a) shows the RF sensor derivative response to soot accumulation on the DPF for two pedal tip-in events along with the AVL measurements [24].

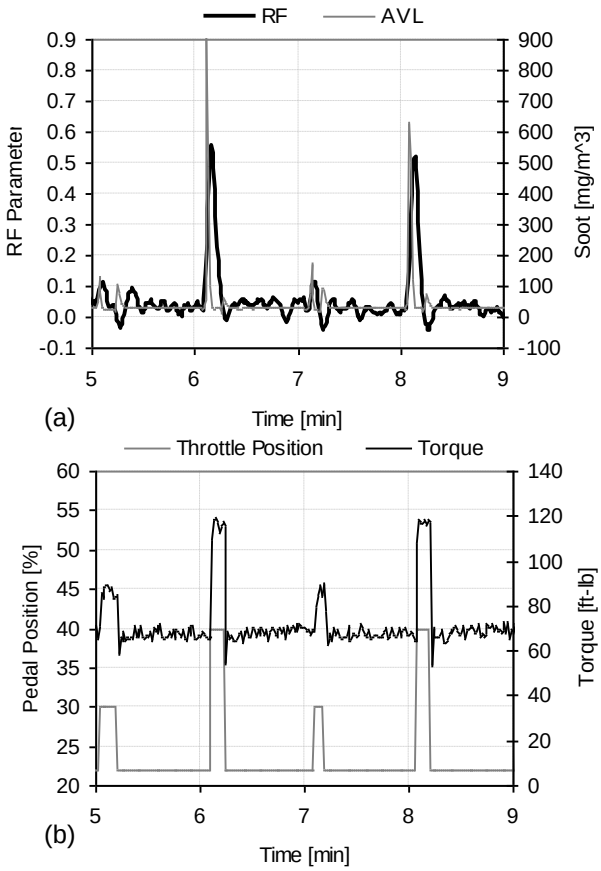

Figure 9. AVL MSS response and derivative of the RF measured DPF soot load (a) for short-duration pedal tip in events at elevated load (b). Images from SAE 2016-01-0918.

The RF sensor derivative response in Figure 9 is determined from the instantaneous soot accumulation levels measured on the DPF. Figure A-2 of the Appendix includes the raw RF measurements of the filter soot loading levels, as well as the derivative response computed from those measurements. In this manner, the fast-response RF sensor measurements of the filter loading state (2.5 Hz in this study) may serve as an indication of engine-out soot levels, with the particulate filter itself essentially serving as an accumulation soot sensor. While the previous work [24] characterized RF sensor response with a fully-intact (healthy) DPF, this study builds on the previous work by exploring the effect of specific filter failure modes on the RF sensor response over a range of operating conditions.

Fleet Vehicle Evaluations

A three year fleet vehicle test was conducted with MY 2009 and 2010 Volvo/Mack trucks operated by the New York City Department of Sanitation (DSNY). The vehicles were equipped with six-cylinder, 11 L, direct injection, Mack MP-7 diesel engines. Depending on calibration, the engine is rated from 325 to 405 Hp (242- 302 kW) at 2,100 rpm and 1,200 to 1,480 lb-ft (1,626 - 2,005 N-m) at 1,200 rpm. All testing was conducted with the engine operating from the stock calibration and control system, with the RF sensor passively monitoring the state of the particulate filter. Results from the first year of fleet testing were reported by the authors in a previous publication [18].

The DPF system for the test vehicles consisted of an un-catalyzed cordierite particulate filter, measuring 12 inches (30.28 cm) in diameter and 12 inches (30.48 cm) in length, for a total filter volume of 22.24L. A thermal regenerator (burner system) installed in the exhaust near the filter inlet was used for active DPF regeneration, given the low-temperature, urban drive cycles over which these vehicles are routinely operated. Figure 10(a) shows the RF sensor installed on the exhaust stack next to the DPF, and Figure 10(b) shows the vertical aftertreatment system configuration on one of the fleet test vehicles.

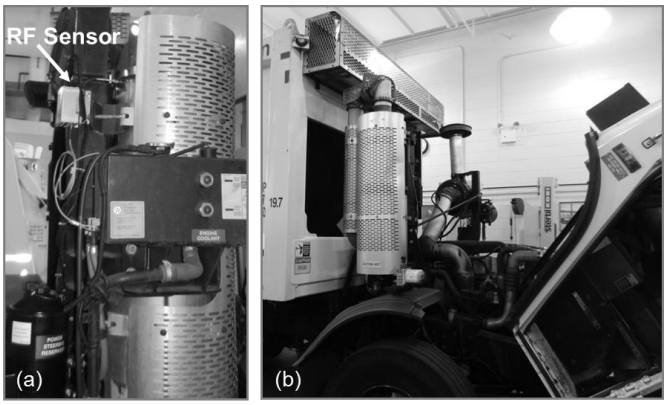

Figure 10. RF sensor installed on exhaust stack of Mack test vehicle (a) and diesel particulate filter configuration and test vehicle (b).

Diesel Engine and Instrumentation

Laboratory testing was also conducted with the RF sensor installed on a 1.9-liter, four-cylinder General Motors (GM) common rail diesel engine coupled to a motoring direct current dynamometer. The engine has a rated power of 110 kW (148 hp) at 4000 rpm and a rated torque of 315 N-m (232 ft-lb) at 2000 rpm. The engine is equipped with a high-pressure common rail fuel injection system, variable geometry turbocharger, swirl actuation, and cooled exhaust gas recirculation (EGR). All experiments were carried out with the engine operating on ultra-low-sulfur certification diesel fuel (Haltermann Solutions).

The RF sensor was installed on a catalyzed cordierite diesel particulate filter, with a 200/12 channel geometry (cell density/wall thickness). The total particulate filter volume was 2.47L. A diesel oxidation catalyst (DOC) was located upstream of the catalyzed DPF. Figure 11 presents a schematic layout of the engine, exhaust system, and RF sensor configuration.

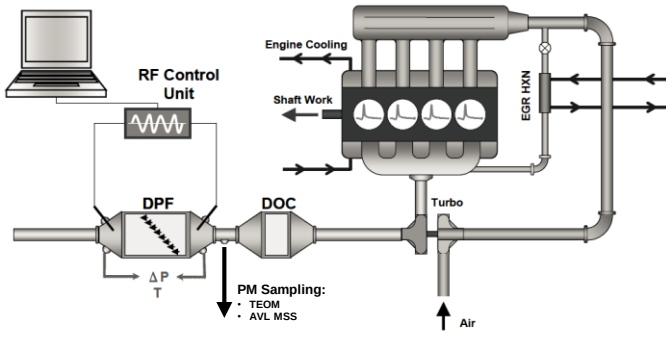

Figure 11. Test setup showing exhaust aftertreatment system configuration and RF measurement system installed on 1.9L GM diesel engine platform.

The factory engine control unit was replaced with a custom full-pass control system developed by National Instruments – Powertrain Controls Group. For the majority of this study, the stock engine parameters were employed; however, a number of engine parameters were modified for custom control strategies specific to this study such as DPF regeneration and engine load "tip-in" experiments.

In the engine load "tip-in" experiments, a step change in engine load was initiated. Changes in engine-out PM emissions were measured by the AVL micro-soot sensor (MSS) and tapered element oscillating microbalance (TEOM) and were then compared to the instantaneous change in the DPF loading state measured by the fast response RF sensor. The AVL MSS provides a continuous measurement, 1 Hz sampling rate, of soot emissions entering or exiting the DPF, depending on sampling location. Similarly, the TEOM provides a direct measurement of total PM mass using a small filter element mounted on a microbalance. The system instrumentation is shown in Figure A-3 of the Appendix. Periodic gravimetric measurements were also conducted to verify filter soot load. Measurements were carried out with fully-intact (healthy) filters as well as filters containing specific intentionally induced defects to reduce the filter's trapping efficiency and simulate specific failure modes.

Gasoline Engine and Instrumentation

Evaluations with the RF sensor and GPF, installed on a gasoline engine, were also conducted at Oak Ridge National Laboratory. The engine used for the evaluations was a BMW N43B20 4-cylinder engine from a MY2008 BMW 120i (E87) vehicle. The engine is a 2.0 liter, naturally aspirated, direct injection, gasoline engine. Figure 12(a) shows the vehicle installed on the chassis dynamometer at ORNL, and Figure 12(b) shows the engine installed on the dynamometer test bed.

Figure 12. MY 2008 BMW 120i vehicle on chassis dynamometer at Oak Ridge National Laboratory (a) and N43B20 4-cylinder lean-burn engine corresponding to the same vehicle, including GPF, setup on the test bed (b).

Similar to the evaluations on the diesel engine, the factory engine control unit was replaced with a custom full-pass control system developed by National Instruments – Powertrain Controls Group. The control system enables full command of the engine operation. Details of the engine specifications are listed in Table 1.

Table 1. BMW N43B20 engine specifications.

Engine Model Number	N43B20
Displaced volume	1995 cm^3
Number of cylinders	4
Number of valves	4 per cylinder
Stroke	90 mm
Bore	84 mm
Compression ratio	12.0:1
Rated Power	125 kW at 6700 rpm
Rated Torque	210 Nm at 4250 rpm

The testing utilized a cordierite gasoline particulate filter, shown installed on the engine in Figure 12(b). The filter measured 5.2 inches in diameter and 5 inches in length, with a cell geometry of 200/8. The RF system utilized two antennas, also shown in Figure 12(b). PM emissions sampling followed the same setup used for the diesel experiments consisting of the AVL MSS and TEOM, as shown in Figure A-3 of the Appendix. Gaseous emissions were also sampled with FTIR and periodic gravimetric measurements of the filter were conducted to verify soot loading levels.

Results and Discussion

Two sets of experiments were conducted in this study in order to evaluate the diagnostic applications of the RF sensor. The first set of evaluations spanned a three-year vehicle fleet test and includes results from filter failure events which occurred during normal vehicle operation in the field. The second set of experiments focused on dynamometer testing with new and damaged filters to quantify the RF sensor response to reduced PM trapping efficiency due to specific filter defects and failure modes.

Diesel Particulate Filter Fleet Evaluations

Normal DPF and RF sensor operation over the course of a three-year vehicle fleet test are described in a previous work by the authors [18]. The testing included a number of heavy-duty vehicles operating on predominantly urban driving cycles in New York City. RF sensors installed on the DPFs were used to passively monitor filter loading levels and state-of-health, while the particulate filter operation (and regeneration) was managed by the stock control system.

An engine malfunction resulting in subsequent catastrophic failure of the DPF is shown in Figure 13. The first 16 hrs of data (from 520 – 536 hrs) show normal DPF operation, with soot loading phases followed by periodic active regeneration events. At hour 536 the RF sensor shows an abnormally high filter soot load (cliff event) which is the result of an upstream engine system malfunction generating high engine-out soot. Despite the high filter soot accumulation, the stock control system does not detect any abnormal operation and the vehicle continues to operate for another 20 hrs until a regeneration is triggered shortly after hour 555.

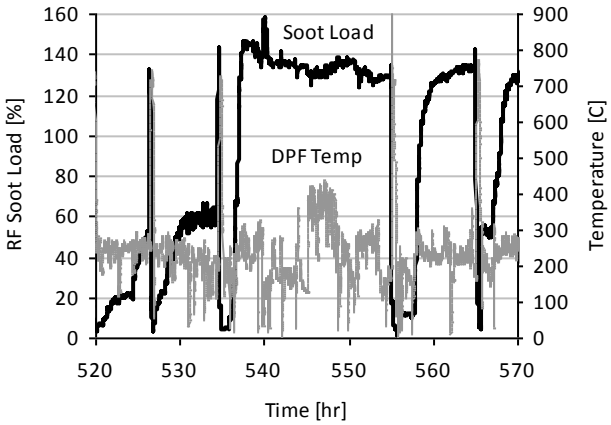

Figure 13. RF sensor measurements of particulate filter soot load, showing upstream engine malfunction detected at hour 536 resulting in abnormally high filter soot loading. Malfunction was detected by the RF sensor 20 hrs before catastrophic DPF failure.

The active regeneration triggered by the stock control system at hour 555 results in an uncontrolled regeneration event. Figure 14 shows the details of this regeneration, whereby rapid soot oxidation, shown by the RF sensor output is observed. Despite filter inlet temperatures measured around 700°C, filter outlet temperatures spike to over 1,000 °C, indicative of high soot load regeneration. It should be noted that the inlet temperature reading on these vehicles generally does read higher than actual filter inlet temperatures, as the inlet thermocouple is mounted near the burner outlet for the active regeneration system.

Despite complete soot oxidation following the active regeneration event shown in Figure 14, the upstream engine malfunction was not corrected for some time. Figure 13, shows the RF sensor repeatedly measuring excessively high filter soot levels following the regeneration event at hour 555, indicating that the problem still persisted and went undetected by the existing diagnostic systems on the vehicle.

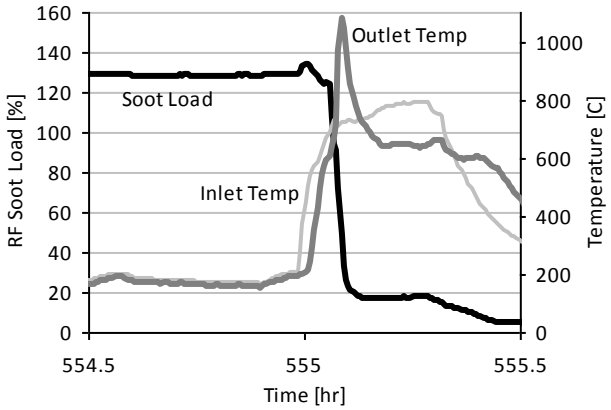

Figure 14. Details of uncontrolled regeneration event resulting in catastrophic DPF failure. Outlet temperatures shown exceeding 1,000 °C.

A post-mortem analysis of the filter removed from the vehicle following the uncontrolled regeneration event shown in Figure 14 was conducted, and several of the borescope images are presented in Figure 15. The images clearly show the melted and damaged channels resulting from the heat released during the regeneration.

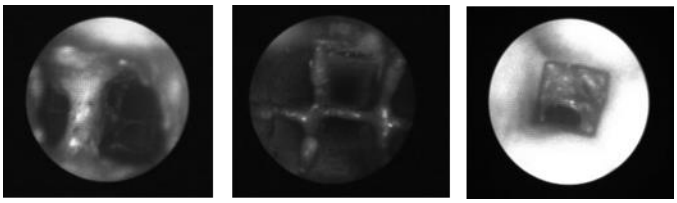

Figure 15. Borescope images showing internally melted regions of failed filter corresponding to the uncontrolled regeneration event shown in Figure 14.

The results of the fleet test provide an important example illustrating the practical application of direct filter state measurements using RF sensing to provide early warning of upstream engine system malfunctions which impact the particulate filter. Such early warning could be implemented to prevent the filter failures, shown in Figure 15, to avoid not only the excess PM emissions associated with the operation of a failed DPF, but more importantly to prevent the failure in the first place.

Diesel Particulate Filter Dynamometer Results

Although the vehicle fleet tests provide real-world, in-use examples of sensor response to detect failure events, laboratory evaluations allow for more precise system characterization under carefully-controlled conditions. The DPF evaluations utilized new and intentionally damaged catalyzed, cordierite particulate filters. In order to simulate failure events resulting in a reduction in filter trapping efficiency (soot slip), an increasing number of ceramic end plugs was removed from the back of the filter. Although not necessarily representative of in-use failure modes, such as those shown in Figure 15, similar approaches have been used to evaluate the sensitivity of soot sensors to meet OBD requirements [25].

Figure 16 illustrates the severity of the failures, which ranged from the removal of only 6 channel end-plugs corresponding to 0.24% of the filter's outlet face area, to the removal of a large 4 inch diameter section of end-plugs corresponding to slightly more than 50% of the filter's outlet face area.

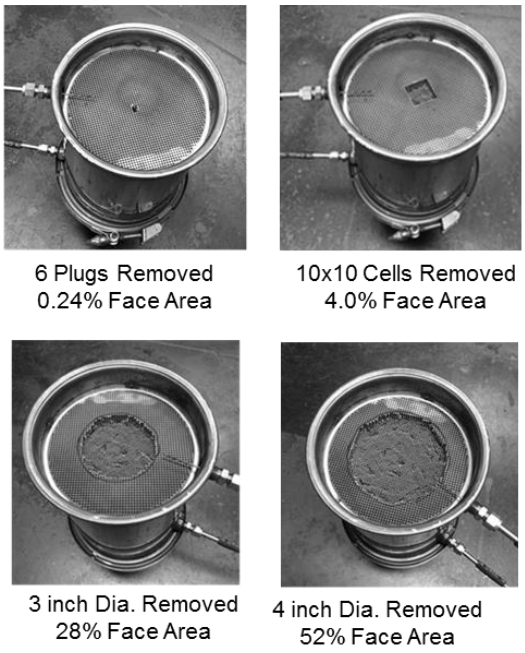

Figure 16. Removal of channel end plugs from rear face of cordierite diesel particulate filter to induce increasing levels of soot slip through the filter.

Each of the filters with the defects noted in Figure 16, was installed on the 1.9L GM turbo-diesel test engine at ORNL. The filters were operated over the same drive cycle, which also included several pedal tip-in events. Figure 17 presents the cumulative results from several tip-in events over the cycle. The RF measurements correspond to the derivative of the RF sensor response to soot accumulation on the filter. The derivative response and raw RF sensor response were previously described in relation to Figure A-2 of the Appendix.

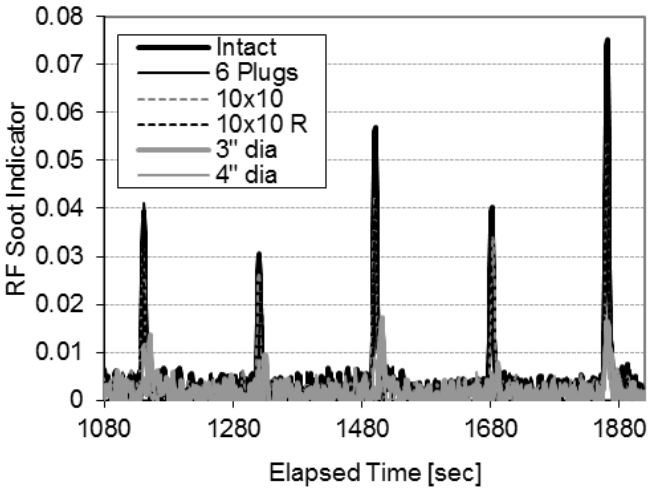

Figure 17. RF sensor derivative response (RF soot indicator) to pedal tip-in events with filters containing varying levels of defects corresponding to the removal of the end plugs shown in Figure 16.

The results presented in Figure 17 show a decrease in the amplitude of the RF sensor derivative signal with increasing size of the filter defect. The derivative response provides a measure of the rate of soot accumulation on the filter, and is expected to decrease as the filter's trapping efficiency decreases due to the removal of the channel end plugs. The highest RF sensor derivative response is

shown for the fully-intact filter exhibiting the highest trapping efficiency for all cases.

Figures 18 and 19 show the details around two of the pedal tip-in events for all five filter test cases. It should be noted that the same test cycle was repeated sequentially with each filter. All efforts were made to synchronize the resulting measurements, however any slight variations in timing of the pedal tip-in events may be due to slight differences in the timing of the tests. A reduction in the RF sensor derivative response is clearly observed in both figures for the case where as few as 6 channel end plugs are removed. The reduction in the derivative response increases with increasing size of the defect.

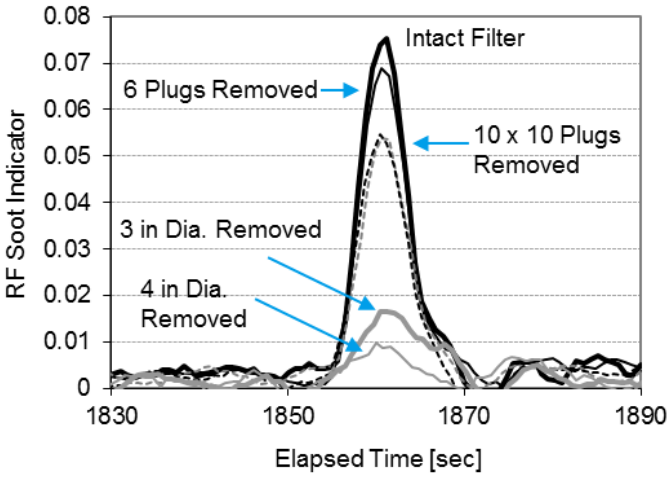

Figure 18. Details of single pedal tip in event showing a significant decrease in the RF sensor derivative signal with increasing soot slip through the DPF.

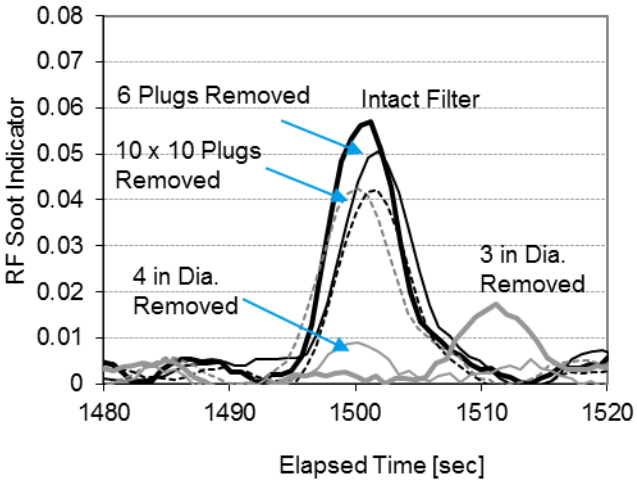

Figure 19. Details of single pedal tip in event showing a significant decrease in the RF sensor derivative signal with increasing soot slip through the DPF.

The case in which a 10 cell x 10 cell square region of end-plugs was removed, corresponding to approximately 4% of the outlet face area of the DPF, was repeated twice. In both cases, Figures 18 and 19 show quite repeatable results for the first and second set of experiments, (denoted 10x10 and 10x10R in Fig. 17) and shown by the dashed lines in Figures 18 and 19.

The results of the measurements shown in Figure 17 were used to evaluate the sensitivity of the RF derivate response to the size of the defect in the filter. Figure 20 presents the RF derivative parameter as a function of the severity of the filter failure. The two repeat test points also show good agreement for the removal of the 10 x 10 square section of channel end-plugs. The results indicate high sensitivity to detect small defects, which are manifested as a measured reduction in PM trapping efficiency relative to the new (un-damaged) filter.

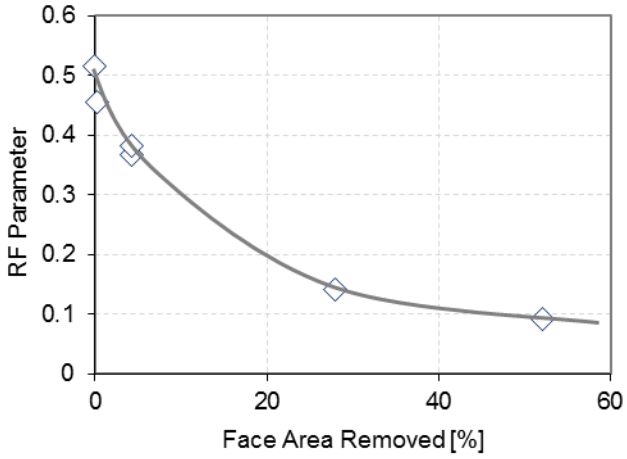

Figure 20. Relative reduction in RF sensor derivative response as a function of increasing filter defect size.

A distinct reduction in the RF sensor derivative response is, thus, well-correlated to a reduction in soot accumulation on the filter and increased tailpipe PM emissions. The measurements are made possible through the fast response of the sensor (2.5 Hz in this study) which enable direct measurements of the filter loading state, even over transient tip-in events, such as those shown in Figures 17-19.

Gasoline Particulate Filter Dynamometer Results

RF sensor evaluations on a BMW lean-burn, direct injection gasoline engine, equipped with a cordierite GPF were also conducted. The general test cycle is shown in Figure 21. As opposed to the pedal tip-in events conducted in the diesel case, variations in exhaust soot concentration were accomplished by modulating the combustion mode between stoichiometric and lean-stratified operation.

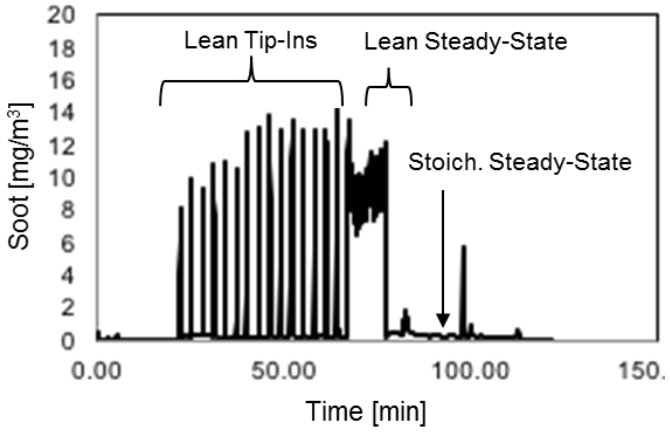

Figure 21. AVL MSS response over the test cycle used for GPF evaluations showing impact of varying combustion mode on engine-out PM emissions.

Figure 21 shows operation with lean-stratified combustion results in increased engine-out PM emissions, relative to stoichiometric

combustion, as measured by AVL MSS. The figure further shows the full test cycle, which consisted of periods of steady-state operation, in addition to modulation of the combustion mode. Details of the AVL MSS response to the lean tip-in sequence are shown in Figure 22 for soot measurements at the engine-out position, with additional details shown in Figure A-4 of the Appendix.

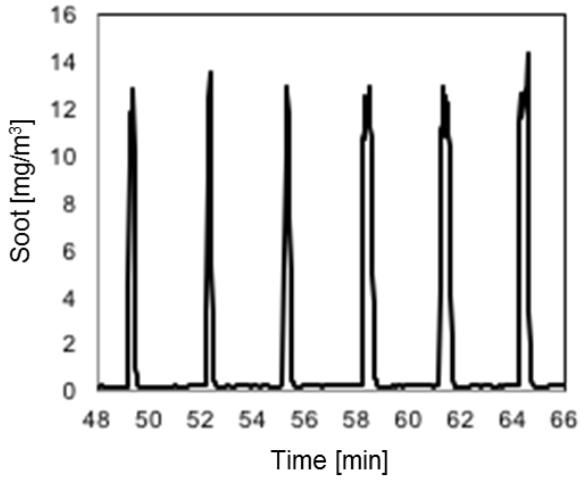

Figure 21. AVL MSS response for lean-stratified combustion mode switching events on BMW lean-burn engine at the engine-out position..

Figure 22 presents results from the AVL MSSS measurements at the GPF-outlet location for the same operating cycle shown in Figure 21 lean-stratified / stoichiometric combustion modulation. Very little response is noted in the AVL MSS signal for the tailpipe measurements with a new (undamaged) GPF.

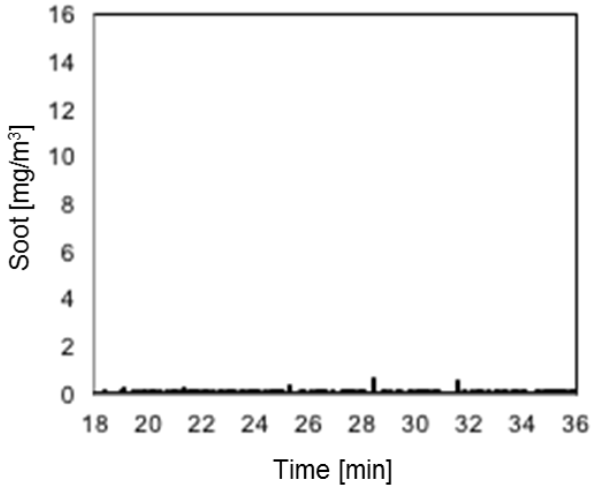

Figure 22. AVL MSS response for lean-stratified combustion mode switching events on BMW lean-burn engine at the GPF-out position with a new, undamaged GPF.

Figures 23 and 24 show the same AVL MSS measurements for the same combustion mode switching events where a small number of channel end-plugs have been removed from the back face of the GPF. In the case of Figure 23, ceramic end-plugs from a region containing 8 cells x 8 cells were removed, and in the case of Figure 24, ceramic end-plugs from a region containing 16 cells x 17 cells were removed.

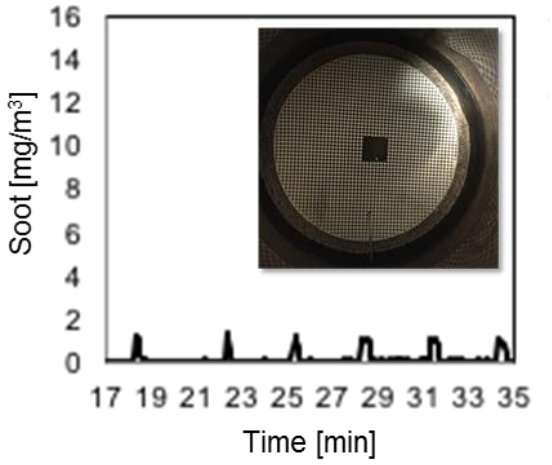

Figure 23. AVL MSS response for lean-stratified combustion mode switching events on BMW lean-burn engine at the GPF-out position where a region containing end-plugs from 8 cells x 8 cells were removed.

Removing channel end-plugs results in additional soot slip through the filter (reduced trapping efficiency) as shown by the measurements in Figure 23 and 24, relative to Figure 22 with an undamaged GPF. Based on the AVL MSS measurements, approximately 9% of the incoming soot escapes the GPF in the case corresponding to Figure 23 where a total of 32 end-plugs were removed. In the case of Figure 24, approximately 136 plugs were removed corresponding to approximately 22% of the incoming soot escaping or slipping through the GPF.

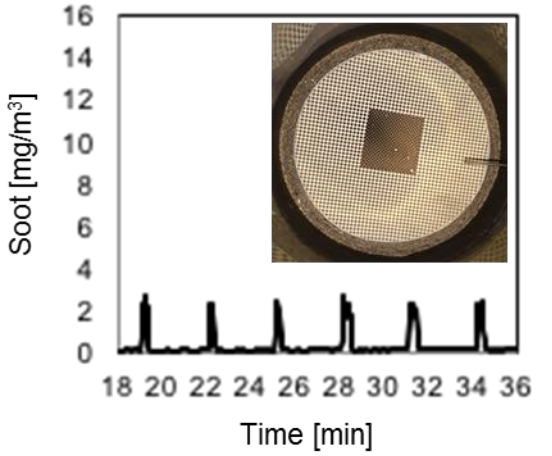

Figure 24. AVL MSS response for lean-stratified combustion mode switching events on BMW lean-burn engine at the GPF-out position where a region containing end-plugs from 16 cells x 17 cells were removed.

The RF measurements corresponding to the GPF tests and failure modes show in Figures 21-24 are presented in Figure 25. For this test campaign an initial RF sensor soot load calibration was developed by loading the GPF to specific soot levels, verified gravimetrically, and correlating RF sensor output to the particulate filter loading levels to establish the calibration function with a new (undamaged GPF). The same calibration function was employed for all of the filter tests, including evaluations with the damaged filter. The results in Figure 25 show small step changes in the measured filter soot load, which correspond to the soot addition associated with each mode switching event. The mode switching events result in periodic increases in engine-out PM as shown in Figure 21.

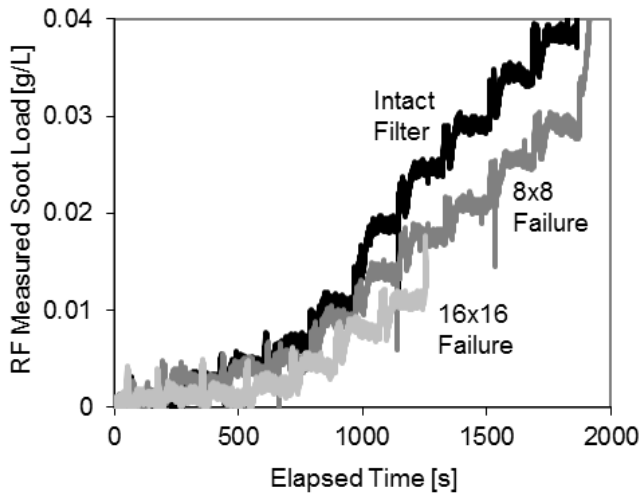

Figure 25. RF sensor measured soot load corresponding to the combustion mode switching events shown in Figures 21-24.

Figure 25 clearly shows a reduction in PM accumulation in the filter for the cases in which end-plugs have been removed from the filter, relative to the undamaged (intact) filter case. The full test cycle was conducted for the case where a region of 8 x 8 cells were removed, however the test where 16 x 16 cells were removed had to be discontinued prior to completion due to an issue with the engine. Nonetheless, the results indicate a lower soot storage on the particulate filter, as measured by the RF sensor, with increasing levels of damage to the filter.

The GPF test cycle further included a brief period of steady state operation, shown in Figure 26. The RF measured soot load shows a steadily increasing signal as PM accumulates on the GPF. Here too, the effect of the damaged filters are to reduce the accumulation rate of soot n the GPF (additional soot slip) as evidenced by the reduction in slope of the measurements with the damaged filters in Figure 26.

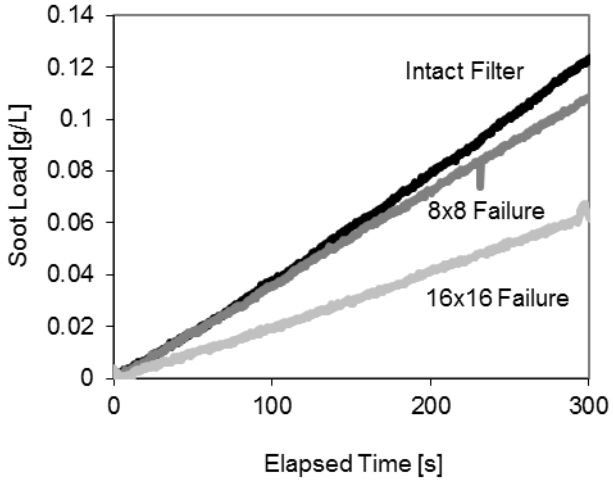

Figure 26. RF response to steady-state soot loading conditions with intact and damaged gasoline particulate filter elements.

Tailpipe measurements with the AVL MSS are shown in Figure 27 corresponding to the test conditions and RF sensor measurements shown in Figure 26. The results confirm an increase in post-GPF soot emissions which is observed to increase with increasing severity of the defects induced to the GPF and are qualitatively consistent with the reduction in trapping efficiency (soot accumulation) on the particulate filter as measured by the RF sensor.

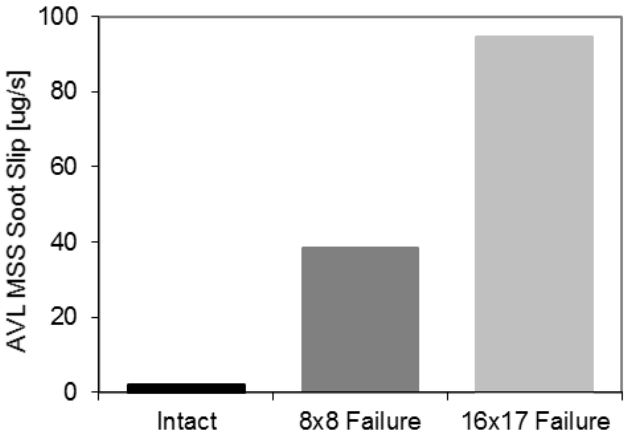

Figure 27. AVL MSS measurements of soot slip through the GPF for the steady-state operating conditions corresponding to Figure 26.

Measurements on a gasoline direct injection engine also confirm the applicability of RF sensing to monitor accumulated PM levels on gasoline particulate filters. In addition a high degree of sensitivity was observed for the RF sensor to detect changes in soot accumulation on the particulate filter, which were well-correlated to the increase in tailpipe soot emissions for damaged filters, as measured by AVL MSS.

Summary and Conclusions

This study applied radio frequency measurements to directly monitor the state of diesel and gasoline particulate filters for on-board diagnostics applications. Fast response RF measurements provide information not only on the health of the particulate filter itself, but also on the upstream processes occurring in the engine which impact particulate filter operation.

Initial bench tests investigated the interaction of the RF resonance signal with the filter media and aftertreatment system housing to determine the sensitivity of the technique to detect the presence of the filter and directly monitor failures or defects to the structure of the filter media itself. The results of the bench tests showed:

- The RF resonances provide a unique signature or reference measurement for an empty filter or catalyst housing. The presence or absence of the filter exerts a large effect on the resonant frequencies, loading the cavity and shifting the resonances to lower frequencies, thereby allowing the presence of the filter to be readily detected. Measurements are possible over all engine operating conditions and may even be conducted with the engine off.

- Defects to the ceramic filter material, including the removal of portions of the filter, are also observed in the RF signal as a shift to higher resonant frequencies. The impact is specific to those resonant modes with associated strong electric fields in the affected region of the filter. Monitoring multiple resonances provides spatial sensitivity to the defects in specific locations of the filter. The magnitude of the defects investigated in the bench tests ranged from 4% to 8% of the total filter volume.

The results of the bench tests clearly indicate the applications of RF sensing to confirm the presence of the ceramic substrate in the filter housing, which can be monitored over the full drive cycle, including with the engine off. Large defects to the filter may also be detected, simulated by the introduction of cuts and the removal of material form specific regions of the filter.

Additional work utilized a combined approach of on-vehicle fleet tests and laboratory dynamometer evaluations with particulate filters installed on diesel and gasoline engines with fast response RF sensors to diagnose the system. The results showed:

- RF sensor measurements may be used to monitor conditions upstream of the particulate filter and detect engine system failures or malfunctions resulting in high engine soot output. Fleet testing with the RF sensor on heavy-duty vehicles detected high soot accumulation on the DPF due to an engine system malfunction (not detected by the stock control system) nearly 20 hours before the stock controller triggered a regeneration which resulted in catastrophic failure to the DPF.

- Laboratory dynamometer testing on a 1.9L GM turbo diesel engine with a catalyzed cordierite particulate filter demonstrated direct measurements of soot slip (manifest through a reduction in soot accumulation) induced by specific filter defects, which were well-correlated with the extent of the damage to the particulate filter. Noticeable reduction in the RF sensor derivative response, related to the soot accumulation rate on the filter, was evident with as few as six end-plugs removed from the back of the filter.

- Evaluations on a 2.0L lean-burn, gasoline direct injection BMW engine equipped with a cordierite gasoline particulate filter further demonstrated high sensitivity of the RF signal to changes in filter trapping efficiency over both transient and steady-state conditions, for filters containing defects of varying severity. The results were consistent with soot slip measured downstream of the GPF by the AVL Microsoot Sensor.

The RF sensing approach investigated in this study provides the potential to detect, with a high degree of sensitivity, signs and symptoms of upstream engine component or subsystem (EGR, turbocharger, injection) malfunctions which impact particulate filter operation. In this manner, early warning may be provided to protect the particulate filter and downstream aftertreatment components from failure. Preventing the failure of the emissions aftertreatment system, not only eliminates the release or escape of emissions above the allowable limits, but also provides significant benefits to the manufacturer and end-user. Furthermore, the bench and engine dynamometer experiments identified additional approaches to either directly or indirectly detect failures or defects in the filter media itself, as well as reductions in filter trapping efficiency in cases where a filter failure has already occurred.

The results, thus, present a paradigm shift in emissions system monitoring and control, by enabling direct measurements of the filter state to preemptively protect and prevent filter failures. The RF measurements may be conducted continuously and with a high frequency, over all operating conditions and drive cycles, including with the engine off, thereby providing a high in-use monitoring rate. Furthermore, should a failure of the filter occur, several means exist for detecting and confirming the failure as well as the reduction in filtering performance of the DPF or GPF.

References

1. Dieselnet, "Emissions Standards, United States: Heavy-Duty On-Road Engines," <www.dieselnet.com>, 2015.
2. Dieselnet, "Emissions Standards, European Union: Heavy-Duty Truck andBus Engines," <www.dieselnet.com>, 2015.
3. Euro 5/6 standards (2009/2014): Regulation 715/2007 and several comitology regulations, http://www.dieselnet.com/standards/eu/ld.php#stds
4. Title 13, California Code Regulations, Section 1968.2, “Malfunction and Diagnostic System Requirements for 2004 and Subsequent Model-Year Passenger Cars, Light-Duty Trucks, and Medium-Duty Vehicles and Engines (OBD II)”, p. 86.
5. European Commission, “Commission Regulation (EC) No 692/2008 of 18 July 2008”, p. L199/94.
6. Rutland, C., Foster, D., Narayanaswamy, K., and He, Y., "Investigation into Different DPF Regeneration Strategies Based on Fuel Economy Using Integrated System Simulation," SAE 2009-01-1275, 2009.
7. Merkel, G., Cutler, W., and Warren, C., "Thermal Durability of Wall-Flow Ceramic Diesel Particulate Filters," SAE Technical Paper 2001-01-0190, 2001, doi:10.4271/2001-01-0190.
8. Yang, K., Fox, J.T. & Hunsicker, R. Emiss. Control Sci. Technol. (2016) 2: 145. doi:10.1007/s40825-016-0036-0
9. Sappok, A., Rodriguez, R., and Wong, V., "Characteristics and Effects of Lubricant Additive Chemistry on Ash Properties Impacting Diesel Particulate Filter Service Life," SAE Int. J. Fuels Lubr. 3(1):705-722, 2010, doi:10.4271/2010-01-1213.
10. Viswanathan, S., Rakovec, N., and Foster, D., “Microscale Study of Ash Accumulation Process in DPF Walls Using the Diesel Exhaust Filtration Analysis (DEFA) System,” ASME ICEF2012-92104, 2012.
11. Iwasaki, S., Mizutani, T., Miyairi, Y., Yuuki, K. et al., "New Design Concept for Diesel Particulate Filter," SAE Int. J. Engines 4(1):527-536, 2011, doi:10.4271/2011-01-0603.
12. Toops, T., Finney, C., Nafziger, E., and Pihl, J., “Neutron Imaging of Advanced Transportation Technologies,” DOE AMR 2013.
13. Masoudi, M., and Sappok, A., "Soot (PM) Sensors," Dieselnet Technology Guide, 2014.
14. Ochs, T., Schittenhelm, H., Genssle, A., and Kamp, B., "Particulate Matter Sensor for On Board Diagnostics (OBD) of Diesel Particulate Filters (DPF)," SAE Int. J. Fuels Lubr. 3(1):61-69, 2010, doi:10.4271/2010-01-0307.
15. Ntziachristos, L., Amanatidis, S., Samaras, Z., Janka, K. et al., "Application of the Pegasor Particle Sensor for the Measurement of Mass and Particle Number Emissions," SAE Int. J. Fuels Lubr. 6(2):521-531, 2013, doi:10.4271/2013-01-1561.
16. Van Nieuwstadt, M., “Monitoring for Gasoline Particulate Filters,” SAE OBD Symposium, 2016.
17. Sappok, A., Bromberg, L., Parks, J., and Prikhodko, V., "Loading and Regeneration Analysis of a Diesel Particulate Filter with a Radio Frequency-Based Sensor," SAE Technical Paper 2010-01-2126, 2010, doi:10.4271/2010-01-2126.
18. Sappok, A. and Bromberg, L., "Radio Frequency Diesel Particulate Filter Soot and Ash Level Sensors: Enabling Adaptive Controls for Heavy-Duty Diesel Applications," SAE Int. J. Commer. Veh. 7(2):468-477, 2014, doi:10.4271/2014-01-2349.
19. Nanjundaswamy, H., Nagaraju, V., Wu, Y., Koehler, E. et al., "Advanced RF Particulate Filter Sensing and Controls for Efficient Aftertreatment Management and Reduced Fuel Consumption," SAE Technical Paper 2015-01-0996, 2015, doi:10.4271/2015-01-0996.

20. Rauch, D., Kubinski, D., Cavataio, G., Upadhyay, D. et al., "Ammonia Loading Detection of Zeolite SCR Catalysts using a Radio Frequency based Method," SAE Int. J. Engines 8(3):1126-1135, 2015, doi:10.4271/2015-01-0986.
21. Moos, R., "Microwave-Based Catalyst State Diagnosis - State of the Art and Future Perspectives," SAE Int. J. Engines 8(3):1240-1245, 2015, doi:10.4271/2015-01-1042.
22. Sappok, A., Ragaller, P., Bromberg, L., Natarajan, G., Warkins, J., and Wilhelm, R., "Particulate Filter Soot Load Measurements using Radio Frequency Sensors and Potential for Improved Filter Management," 2016, 2016-01-0943.
23. Sappok, A., Bromberg, L., "Development of Radio Frequency Sensing for In-Situ Diesel Particulate Filter State Monitoring and Aftertreatment System Control," ASME ICEF2013-19199, ASME ICED Fall Technical Conference, April 2013.
24. Sappok, A., Ragaller, P., Bromberg, L., Prikhodko, V. et al., "Real-Time Engine and Aftertreatment System Control Using Fast Response Particulate Filter Sensors," SAE Technical Paper 2016-01-0918, 2016, doi:10.4271/2016-01-0918.
25. Kondo, A., Yokoi, S., Sakurai, T., Nishikawa, S. et al., "New Particulate Matter Sensor for On Board Diagnosis," SAE Int. J. Engines 4(1):117-125, 2011, doi:10.4271/2011-01-0302.

Contact Information

Dr. Alexander Sappok: alexander.sappok@ctscorp.com

Acknowledgments

This material is based upon work supported by the U.S. Department of Energy DE-EE0005653. The authors would like to thank Roland Gravel, Ken Howden, and Gurpreet Singh from the DOE and Ralph Nine from NETL for their support and engaging discussions.

Definitions/Abbreviations

ATDC	After Top Dead Center
DOC	Diesel Oxidation Catalyst
DPF	Diesel Particulate Filter
ECU	Engine Control Unit
GPF	Gasoline Particulate Filter
MAF	Manifold Air Flow
MSS	Micro Soot Sensor
OBD	On-Board Diagnostics
PM	Particulate Matter
RF	Radio Frequency
SCR	Selective Catalytic Reduction
TEOM	Tapered Element Oscillating Microbalance
TWC	Three-Way Catalyst

Appendix

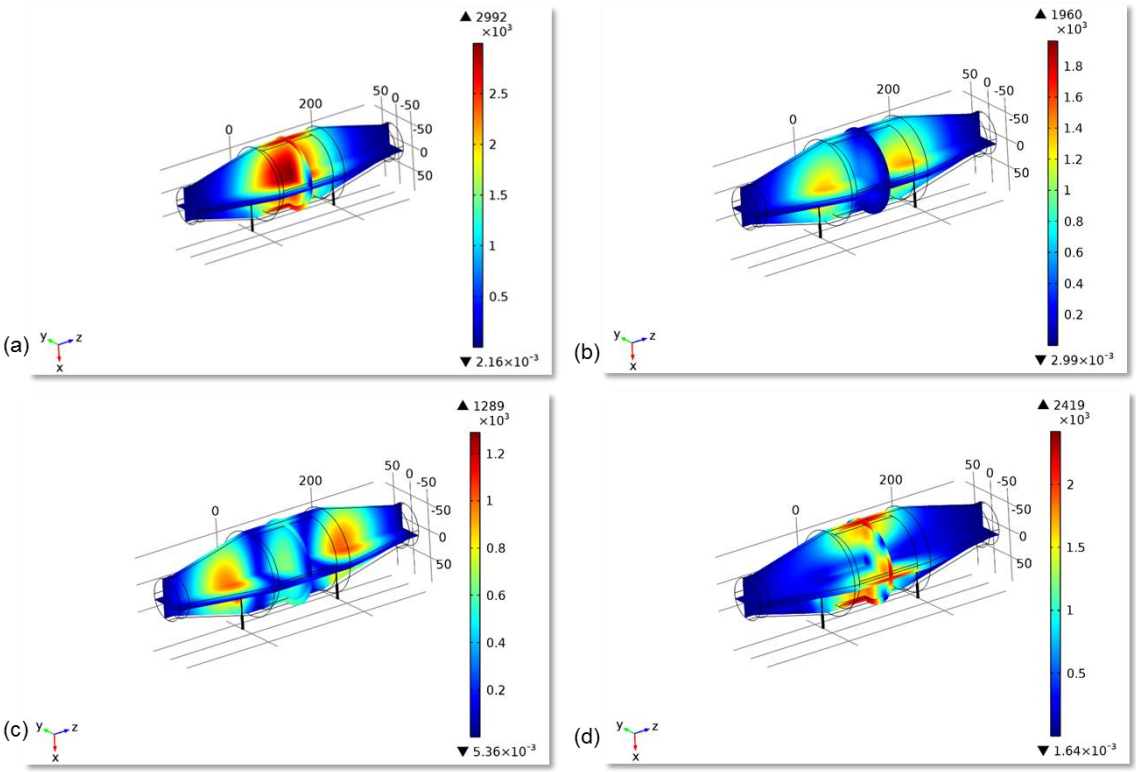

Figure A-1. Simulation results showing electric field distribution of several resonance modes (a) – (d) for a cordierite gasoline particulate filter. Red and orange regions indicate local areas of high field strength within the filter housing. Fundamental mode is shown in (a) indicating a high field in the center of the filter. Higher order modes (c) and (d) show axial variation in the electric field and mode (d) shows radial variation. Regions of high electric field correspond to resonances with high sensitivity to monitor changes occurring on the filter in those regions.

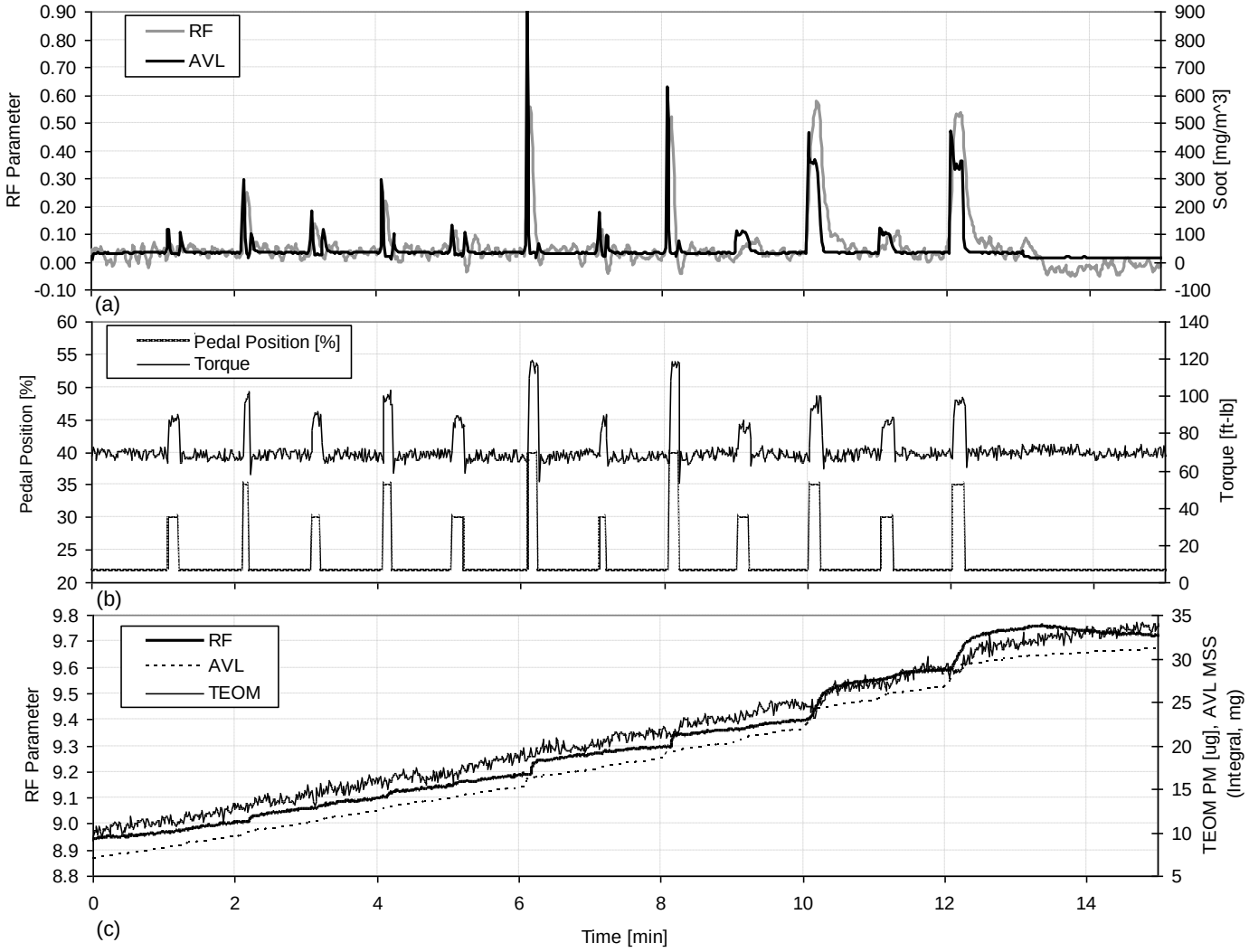

Figure A21. Summary of pedal tip-in experiments showing AVL MSS response and derivative of RF sensor response (a), engine pedal and load conditions (b) and raw RF sensor response to DPF soot accumulation, TEOM output, and integrated AVL MSS signal (c). Reproduced from [24].

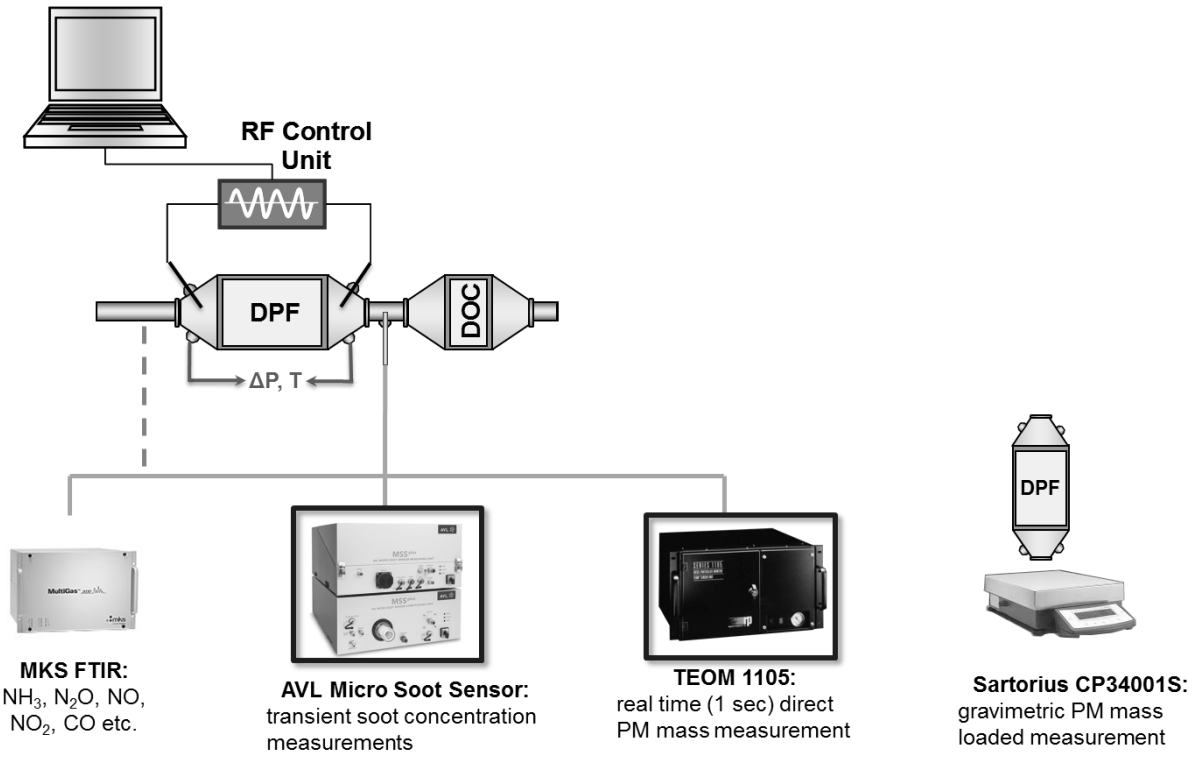

Figure A-3. System instrumentation for PM and gaseous emissions measurements sued for the diesel and gasoline engine testing at Oak Ridge National Laboratory.

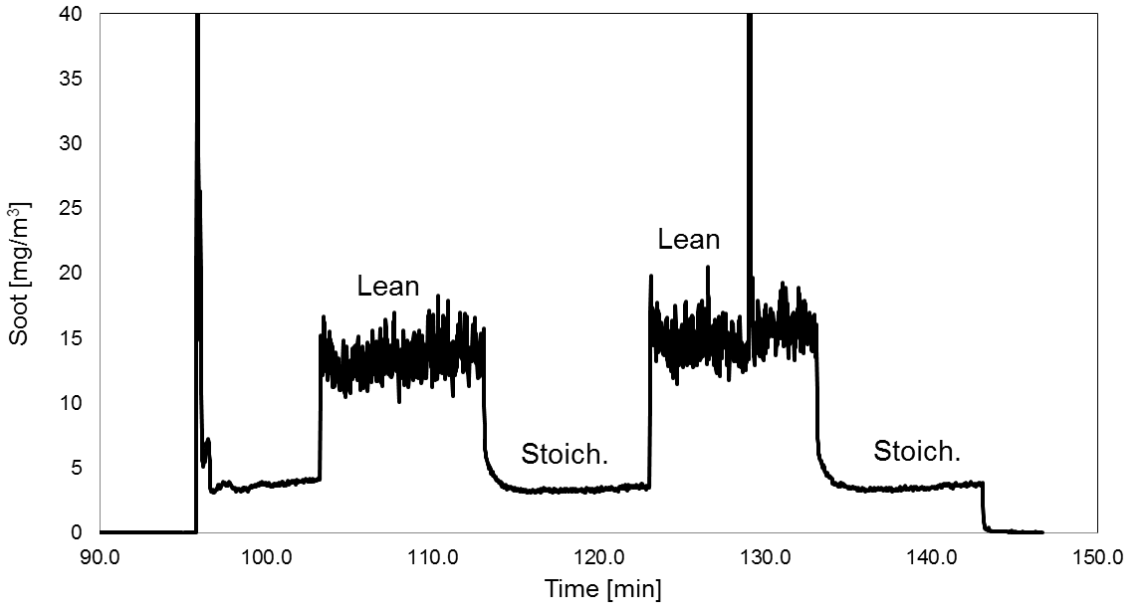

Figure A-4. Detail of AVL MSS measurements for mode switching events between lean stratified operation and stoichiometric operation on BMW direct injection gasoline engine.